Planting *Cyperus esculentus* augments soil microbial biomass and diversity, but not enzymatic activities

Yulong Duan[a, b, #, *]**, Wei Ren**[c, #]**, Jianhua Zhao**[d]**, Chun Luo**[d]**, Yang Liu**[e]

[a] *Northwest Institute of Eco-Environment and Resources, Chinese Academy of Sciences, Lanzhou 730000, China.*

[b] *Naiman Desertification Research Station, Northwest Institute of Eco-Environment and Resources, Chinese Academy of Sciences, Tongliao 028300, China.*

[c] *Agricultural Biotechnology Institute, Jilin Academy of Agricultural Sciences, Changchun 130033, China.*

[d] *Shanghai Majorbio Bio-pharm Technology Co., Ltd, Shanghai 200120, China.*

[e] *Gansu Institute of Architectural Design and Research Company, Lanzhou 730000, China.*

[#] Co-first authors who contributed equally to this work (Y. Duan and W. Ren).

*Corresponding author Northwest Institute of Eco-Environment and Resources, Chinese Academy of Sciences, 320 Donggang West Road, Lanzhou 730000, China (Y. Duan).

E-mail address: duanyulong@nieer.ac.cn (Y. Duan); renwei@cjaas.com (W. Ren).

Abstract

The planting of *Cyperus esculentus*, a member of the grass family *Cyperaceae* which includes nut sedge weeds, is being increasingly promoted in northern China's semi-arid and arid regions. Yet the effects of planting *C. esculentus* upon soil quality and soil microbial characteristics of sandy land remain unclear. This study examined the short-term (1 year) impact of this grass species on soil microbial biomass indices, enzymatic activities, and microbiome characteristics in the Horqin Sandy Land area of China. The results show that planting *C. esculentus* could increase microbial biomass in the form of carbon (MBC), nitrogen (MBN), and phosphorus (MBP), but it negligibly influenced the enzymatic activities of soil β-1,4-glucosidase (BG), cellobiohydrolase (CBH), leucine aminopeptidase (LAP), and β-1,4-N-acetaminoglycosidase (NAG). Over 1 year, we found that planting *C. esculentus* significantly increased the soil bacterial richness and diversity of sandy land, yet also altered community composition of soil bacteria and eukaryotes in way that could promote their homogenization. In this respect, the relative abundances of *Acidobacteria* and *Proteobacteria* significantly decreased and increased, respectively; hence, they may be considered for use as important indicators of soil nutrient-rich conditions. Overall, the results could be explained by greater soil organic carbon (SOC) and total nitrogen (TN), mainly derived from cumulative plant litter input to soils, which then increased the sandy soil's C:N ratio. Future research should focus on exploring the long-term effects of planting *C. esculentus* on soil quality and soil microbial characteristics of sandy lands in China and abroad.

Keywords: *Cyperus esculentus*, soil microorganisms, soil organic carbon, soil enzymatic activities, semi-arid and arid regions

1. Introduction

41

42   *Cyperus esculentus*, also known as chufa sedge, yellow nut sedge, tiger nut sedge, or earth almond,

43   belongs to the grass family *Cyperaceae*. This plant species is a perennial weed native to the

44   Mediterranean region, but has since spread globally, in part because of its well-developed root system,

45   strong tillering ability, short growing period, large biomass, high oil content, strong resistance to stress,

46   and a wide range of adaptive traits. Nevertheless, the tubers of *C. esculentus* are valued for their health

47   and nutritive benefits (Asare et al., 2020; Oderinde and Tairu, 1988), and in recent years, the distribution

48   of introduced *C. esculentus* has extended considerably in the semi-arid and arid regions of northern China.

49   There, the total cultivated area of *C. esculentus* reached 6886 km² in 2021, mainly in the Inner Mongolia

50   Autonomous Region, Xinjiang Uygur Autonomous Region, Liaoning Province, and Jilin Province, whose

51   coverage is expected to continue expanding (Sha et al., 2022; Zhang and Wu, 2022). In these regions, *C.*

52   *esculentus* is generally grown on sandy soil or sandy loam to conveniently harvest its valued tuberous

53   roots, given the typically loose texture of sandy land. Surprisingly, however, the effects of planting *C.*

54   *esculentus* on the soil quality of sandy land and its soil microbial characteristic are still poorly understood.

55   Soil microbes are indispensable components of terrestrial ecosystems and their biological

56   characteristics, including diversity, community composition, biomass, quantity, and enzymatic activity,

57   are highly sensitive to changing environmental conditions (Hu et al., 2019; Lange et al., 2015; Neilson et

58   al., 2012; Yu et al., 2022). A meta-analysis of 81 available studies from 28 countries indicates that plant

59   crops enhance soil microbial diversity and biomass, and altered community structure compared to no

60   plant crop, and the responses of microbial parameters to plant crop varied with soil and climatic

61   conditions (Muhammad et al., 2021). Actually, such soil microbial biological characteristics can more

62   directly engage in feedback with altered soil quality than can physicochemical properties such as soil

63   organic matter (SOC) and soil nutrient content (Bünemann et al., 2018; Caldwell, 2005). Microbial

64   biomass, namely microbial biomass in terms of carbon (MBC), nitrogen (MBN), and phosphorus (MBP)

65   is the main driving force behind the transformation and cycling of soil organic matter and nutrients (N

66   and P); it is also functions as a crucial reserve pool for soil nutrients to provision plants' growth, and can

67   thus serve as an indicator of soil fertility (Jenkinson and Ladd, 1981; Pan et al., 2018; Powlson et al.,

68   2001; Sparling et al., 1997). Soil extracellular enzymes are special secondary metabolites secreted by

69   microorganisms to obtain energy and nutrients from soil. Accordingly, changed extracellular enzymes

70   activities may reflect the metabolic status of a soil microbe taxon or community as well as the potential

71   for specific soil biochemical reactions (Dirks et al., 2012; Ma et al., 2022). Notably, in response to sudden

72   changes in environmental conditions, soil extracellular enzymes are often expressed and released, such as

73   β-1,4-glucosidase (BG), β-1,4-N-acetylglucosaminidase (NAG) and leucine aminopeptidase (LAP), acid

74   phosphatase (ACP); these have been used to successfully characterize the cycling dynamics of carbon (C),

75   nitrogen (N), and phosphorus (P) in soil, respectively (Allison and Jastrow, 2006; Brunner et al., 2003;

76   Shao et al., 2020). In particular, cellobiohydrolase (CBH) are a class of key enzymes functioning in

77   cellulose hydrolysis and biomass conversion, which may be used to characterize the decomposition

78   capacity of cellulose material (Haan et al., 2013).

79   The sandy land of semi-arid and arid ecosystems is generally characterized by low microbial

80   biomass indices, enzymatic activities, and α-diversity, these features usually ascribed to its low soil

81   moisture and poor availability of limiting nutrients. Therefore, we hypothesized that planting *C.*

82   *esculentus* followed by its growth (cultivation) for 1 year would increase the soil microbial biomass,

83   richness, and diversity. Our study's findings provide timely scientific data to inform future strategies for

84   planting *C. esculentus* on sandy soils in the semi-arid areas of northern China.

85

86   2. Materials and methods

87   *2.1 Site description and soil sampling*

88   The two sampling sites were established, one on bare sandy land (*BSL*) and the other on sandy land

89   in which *C. esculentus* was planted and cultivated for 1 year (*CE*) (Fig. S1). Both experimental sites were

90   located in Naiman, Tongliao, of Inner Mongolia, in a semi-arid region of China's Horqin Sandy Land

91   (42°55′N, 120°42′E; 348 m a.s.l.). This region has a continental semi-arid monsoon temperate climate,

92   with a mean annual temperature of 6.8°C and a mean annual precipitation of 360 mm, 70% of which

93   occurs from May through September. The dominant native plant species of the sandy land were *Caragana*

94   *microphylla*, *Setaria viridis* and *Echinops gmelinii*, with a low vegetation cover of 30%. The distance

95   between these two sites is less than 500 m and they were freshly reclaimed in December 2020. The soil

96   type is degraded sandy chestnut soil and aeolian sandy soil, and the topsoil (depth: 0–20 cm) was taken

97   for nutrient determination before reclamation. The soil organic carbon content was 2.61 g·kg^{-1}, soil total

98   nitrogen content was 0.20 g·kg^{-1}, the available phosphorus content was 0.71 g·kg^{-1}. It is characterized by

99   high sand content, low nutrient content and poor water and fertilizer retention.

100   In this study, *C. esculentus* were sown by mechanical seeding method in mid-May. To control for the

101   disturbance caused by fertilization and irrigation, both sites received the same fertilization and irrigation

102   application (urea, 675 kg·hm^{-2}; $(NH_4)_2 \cdot HPO_4$, 300 kg·hm^{-2}; K_2SO_4, 375 kg·hm^{-2}; humid acid, 300 kg·hm^{-2};

103   total irrigation volume was 5800 m^3·hm^{-2}). Of these, the base fertilizer applied before planting (urea, 45

104   kg·hm^{-2}; $(NH_4)_2 \cdot HPO_4$, 300 kg·hm^{-2}; K_2SO_4, 375 kg·hm^{-2}; humid acid 300kg·hm^{-2} and the irrigation

105   amount before sowing was 2025 m^3·hm^{-2}. After that, all treatments adopted the water-fertilizer integration

106   technology for trickle irrigation and fertilization, and the trickle irrigation belt was laid along the planting

107   direction of *C. esculentus*, with an interval of 30 cm for each trickle irrigation belt. At the initial stage of

108   growth (from May to June), water was dropped 4 times, each time 187.5 m^3·hm^{-2}, each hectare 33.75 kg

109   urea and 15 kg K_2SO_4. In the middle irrigation period (from June to mid-August), 12 drops were applied,

110   and in the late irrigation period (from mid-August to mid-September), 4 drops were applied, with the

111   same amount of water and fertilizer per drop as in the initial irrigation period.

112   A total of 10 plots were set up, evenly split between the *BSL* and *CE* sites (i.e., 5 plots per site), and

113   each plot randomly distributed on the *BSL* and *CE sites* (the distance between the plots is ca. 50 m). An

114   auger (2.5-cm diameter) was used to collect topsoil samples (depth: 0–20 cm) on 28 August 2021, this

115   corresponding to the peak of the growing season at *CE*. Within each plot (1 m × 1 m), five random

116   locations were sampled and mixed together to generate a single composite soil sample; all such samples

117   were then individually packed in sterilized polyethylene bags and taken to the laboratory in coolers

118   (portable car refrigerators) as quickly as possible. Any surface litter in the soil samples was removed by

119   passing them through a 2-mm square-aperture mesh. Each composite soil sample was divided into two

120   subsamples: one was stored at 4°C to later determine the soil properties, and the other was stored at –

121   80°C until the DNA extractions.

122

2.2 Measurement of soil microbial biomass carbon, nitrogen, and phosphorus contents

A routine fumigation-extraction methodology was employed to measure the microbial biomass carbon (MBC), nitrogen (MBN), and phosphorus (MBP) (Joergensen, 1996). Briefly, triplicate fresh 50-g soil subsamples were placed separately in 100-mL beakers and incubated in the dark for 7 days at 25°C with a relative humidity (RH) of 70%. The first subsample was set as the control group and the second one fumigated for 24 h with ethanol-free $CHCl_3$; the third one was used to quantify the soil moisture content. The control and fumigated samples were transferred into 250-mL Erlenmeyer flasks, to which 100 mL of 0.5 M K_2SO_4 (for MBC and MBN) or $NaHCO_3$ (for MBP) was added to each, and the solution shaken for 30 min at 25°C to obtain the soil extracts. These extracts were filtered through 0.45-μm cellulose filters and stored at –20°C until their analysis. The MBC, MBN, and MBP contents were all measured using an Elementar Vario TOC (Elementar, Langenselbold, Germany). The MBC, MBN, and MBP were respectively calculated as the difference between the extractable C, N, and P contents of fumigated and control samples, using fixed conversion factors: 0.45 for both the K_{EC} of C and K_{EN} of N, while the K_{EP} for P was 0.40.

137

2.3 Measurement of five types of soil enzymatic activity

For soil enzymes β-1,4-glucosidase (BG), cellobiohydrolase (CBH), leucine aminopeptidase (LAP), β-1, 4-N-acetaminoglycosidase (NAG), and acid phosphatase (ACP), their respective activity was quantified using commercial enzyme kits and following the manufacturer's protocol (Solarbio, Beijing, China). Briefly, BG decomposes p-nitrobenzene-β-D-glucopyranoside, yielding p-nitrophenol; CBH decomposes nitrobenzene fibrodiglycoside (PNPC), yielding p-nitrophenol; LAP decomposes L-leucine-p-nitroaniline, yielding p-nitroaniline; NAG decomposes p-nitrobenzene β-N-acetylglucosamine, yielding p-nitrophenol; and ACP decomposes disodium phenyl phosphate hydrate to yield phenol and Na_2HPO_4. The maximum absorption peak for BG, CBH, or NAG occurs at 400 nm, for LAP at 405 nm, and for ACP at 660 nm; to measure absorbance, a UV-VIS spectrophotometer was used (UV-1800, Mapada Instruments Co., Shanghai, China).

149

2.4 Soil DNA extraction and quantitative PCR

150

151   Soil total DNA was extracted from a 0.5-g subsample using the PowerSoil kit (Omega Laboratories

152   Inc., Mogadore, OH, USA) according the manufacturer's instructions. The integrity of DNA was checked

153   by electrophoresis in 1.0% agarose gel, and its purity and concentration measured spectrophotometrically

154   by a NanoDrop ND5000 (Thermo Fisher Scientific Inc., USA). Next, PCR was conducted in a Line Gene

155   9600 Plus Cycler (Thermo Fisher Scientific Inc.) to amplify the hyper-variable 460-bp V3–V4 region of

156   the 16s rRNA, using the primer pair Eub338/806 (338F, 5'-ACTCCTACGGGAGGCAGCAG-3' (Dennis

157   et al., 2013); 806R, 5'-GGACTACHVGGGTWTCTAAT-3'). Likewise, the 300-bp V5–V7 region of 18

158   rRNA   was   amplified   using   the   primer   pair   SSU0817/1196   (0817F,   5'-

159   TTAGCATGGAATAATRRAATAGGA-3'; 1196R, 5'-TCTGGACCTGGTGAGTTTCC-3') (Rousk et al.,

160   2010).

161   Real-time quantitative PCR (qPCR) was carried out with 25 mg of the DNA mixed with 12.5 mL of

162   ChamQ SYBR color qPCR Master Mix (2x) (Vazyme Biotech Co., Ltd, Nanjing, China), 0.5 mL of a

163   buffer solution (10 mM) of the primer pair, and 9.5 mL of dd H_2O. Standard and environmental DNA

164   samples were added at 2.0 mL per reaction. Every reaction was run on an ABI7300 unit (Applied

165   Biosystems, USA) with this cycling program: initial denaturation at 95°C for 3 min, followed by 40

166   cycles of 94°C for 30 s, 53°C for 30 s, and 72°C for 45 s, with a final extension at 72°C for 5 min (Niu et

167   al., 2021). Melting curve and gel electrophoresis analyses were used to confirm that the amplified

168   products were of the appropriate size. Bacterial and fungal gene copy numbers were generated using a

169   regression equation for each assay that related the cycle threshold (CT) value to a known number of

170   copies in a given standard. All qPCR reactions were run in triplicate for each soil sample. The average

171   bacterial PCR efficiency was 101.00%, with an R^2 of 0.9992 for the standard curves; the fungal PCR

172   efficiency was 105.56% with an R^2 of 0.9999 for the standard curves.

173

2.5 High-throughput amplicon sequencing bioinformatics analysis

174

175   Each PCR was carried out in triplicate, in a 20-μL reaction volume that contained 4 μL of a 5×

176   reaction buffer, 4 μL of dNTPs (2.5 mM), 0.8 μL of each primer (5 μM), 1 μL of template DNA (ca. 10

177   ng), and 0.4 μL of Pfu DNA Polymerase (TransStart-FastPfu DNA Polymerase, TransGen Biotech,

178   Beijing, China), topped up with double-distilled H_2O. The PCR program consisted of an initial

179   denaturation phase at 95°C for 3 min; followed by 35 cycles at 94°C for 30 s, annealing at 55°C for 30 s,

180   and an extension at 70°C for 45 s; a final extension was done at 72°C for 10 min. The PCR was

181   performed in an ABI GeneAmp 9700 Cycler (Thermo Fisher Scientific Inc.).

182   Unique barcode sequences were added at the 5′ end of the forward primer, to separate corresponding

183   reads from the data pool generated in a single sequencing run. The ensuing amplicons were extracted by

184   electrophoresis in 2.0% agarose gel and purified with a Gel Extraction Kit (Axygen Co., Hangzhou,

185   China), according to the manufacturer's instructions, then quantified with a QuantiFluor-ST fluorimeter

186   (Promega, Fitchburg, WI, USA). The purified amplicons were pooled in an equimolar way and paired-end

187   sequenced (2 × 300 bp) by Majorbio Co. Ltd. (Shanghai, China), according to recognized protocols.

188   Raw FASTQ files were de-multiplexed and quality-filtered, by using the 'fastp' tool (v.0.20.0)

189   (Chen et al., 2018) according to these criteria: (i) The 300-bp reads were truncated at any site that had an

190   average quality score < 20 over a 50-bp sliding window, discarding any truncated reads shorter than 50-

191   bp; (ii) Extracted matching barcodes were removed, and as well as any two-nucleotide mismatches vis-à-

192   vis the primer, or reads that contained ambiguous characters; (iii) Overlapping sequences > 10 bp in

193   length were assembled according to their overlapping sequence. Reads that could not be assembled were

194   discarded.

195   The resulting quality-checked sequences were aligned as per the SILVA alignment database

196   (https://www.arb-silva.de) (Quast et al., 2013), and clustered into operational taxonomic units (OTUs) by

197   USEARCH software (v. 7.1) (https://www.drive5.com/usearch/) (Edgar, 2013). Only those OTUs with at

198   least a 97% similarity level were used to draw the rarefaction curves, and the α-diversity indices—Chao,

199   ACE, Shannon, and Simpson indices (http://www.mothur.org/wiki/Calculators), and their performed

200   coverage analysis—were calculated using Mothur software (v1.30.2) (https://www.mothur.org) (Schloss

201   et al., 2009). The taxonomic assignment of OTUs at a 97% similarity cut-off was conducted by Mothur,

202   with a 70% confidence interval, in accordance with the SILVA (138) or Unite (8.0) database

203 (http://unite.ut.ee/index.php) for bacteria and eukaryota, respectively.

204  All sequencing data associated with this study can be found in the NCBI Sequence Read Archive

205 (https://www.ncbi.nlm.nih.gov/sra), under project accession no. PRJNA836307.

206

207 ***2.6 Statistical analysis***

208  Significant differences in the means of soil microbial biomass indices, enzyme activity, quantity, and

209 α-diversity between two sites (*BSL* vs. *CE*) were determined by one-way analysis of variance (ANOVA).

210 All analyses were implemented in SPSS statistical software (v. 19.0)

211 (https://www.ibm.com/analytics/spss-statistics-software). Unless otherwise noted, a difference between

212 means was consider statistically significant at $P < 0.05$. Principal co-ordinates analysis (PCoA) was used

213 to uncover differences in β-diversity between samples of the two sites (*BSL* vs. *CE*). Mantel tests were

214 used to evaluate the relationships of the bacterial or eukaryotic community composition to measure site-

215 level soil variables. Pearson correlation coefficient (r) were used to indicating a positive correlation (r>0)

216 or a negative correlation (r<0). Both PCoA and Mantel tests were carried out in the R platform (v3.2.1)

217 (www.r-project.org) with its 'vegan' package. This package was also used to build the matrices for the

218 pairwise taxonomic distances between the bacterial or eukaryotic communities (Bray–Curtis's

219 dissimilarity) and environmental variables (Euclidean distance). Pearson correlation analysis was carried

220 out in the R platform (v3.2.1) (www.r-project.org) with its function cor ().

221

3. Results

223 ***3.1 Comparative analysis of soil microbial biomass indices and enzymatic activities***

224  The soil biomass microbial indices for the two sites are shown in Fig. 1A. Evidently, the mean

225 values for MBC, MBN, and MBP were one-third to three times greater at *CE* than *BSL*. ($P < 0.05$) (Table

226 S1, Table S3). For the soil MBC:MBN ratio, its mean (± SD) was 18.293 ± 6.868 at *BSL*, which was

227 significantly higher than the 8.324 ± 4.700 at *CE* ($P < 0.05$) (Table S1, Table S3). In Fig. 1B are the soil

228 enzymatic activities (BG, CBH, LAP, NAG, and ACP) for the two sites. In this respect, only ACP

229 differed significantly between BSL and CE, being almost 20% lower in the latter ($P < 0.05$) (Table S2,

230   Table S3).

231

232   ***3.2 Microbial diversity characterization and community composition of the two sites***

233   Gene copy numbers for total bacteria (16S RNA) and eukaryota (18S RNA) species at the two

234   sampling sites are presented in Fig 2. For bacteria, copy abundance was nearly two times higher in the *CE*

235   than *BSL* soil ($P < 0.05$), while the eukaryota were similarly abundant between the two sites ($P < 0.05$).

236   Fig. 3 shows the two α-diversity indexes, community species richness (Chao 1 index) and community

237   diversity (Shannon index), at the two sites. For bacteria, the Chao1 index ranged from 2329.50 to 2677.07

238   and 2690.12 to 2799.07 at *BSL* and *CE*, with means of ca. 2500 and 2700, respectively (Table S4), while

239   the Shannon index ranged from 5.76 to 6.45 and 6.33 to 6.42 respectively at *BSL* and *CE*, also with

240   similar means (Table S4). For eukaryota, the Chao1 index ranged from 73.00 to 110.5 and 83.88 to 117.6

241   at *BSL* and *CE*, with means of ca. 90 and 97, respectively (Table S5); corresponding values for the

242   Shannon index were.10 to 2.73 and 2.16 to 2.55, with nearly identical means (Table S5). The plot-level

243   *ACE* and Simpson indices for the diversity of bacteria and eukaryota are summarized in Tables S4 and S5,

244   respectively.

245   Across all 10 soil samples, a total of 272 464 valid sequences and 4 379 OTUs were obtained. All

246   sequences could be assigned to one of 36 bacterial phyla. Of these, the 19 most dominant bacterial phyla

247   across all samples were *Actinobacteria* (8.01%–12.64%), *Acidobacteria* (5.90%–17.92%), *Proteobacteria*

248   (7.21%–14.38%), *Chloroflexi* (6.55%–12.26%), *Gemmatimonadota* (6.05%–13.09%), *Firmicutes*

249   (6.96%–12.07%), *Bacteriodetes* (7.17%–12.39%), *Myxococcota* (7.46%–13.81%), *Cyanobacteria*

250   (0.69%–32.44%), *Methylomirabilota* (2.84%–18.56%), *Nitrospirae* (5.88%–16.48%),

251   Bacteria_unclassified or norank (4.46%–15.02%), *Patescibacteria* (3.01%–15.39%), *Planctomycetota*

252   (6.45%–14.72%), *Verrucomicrobiota* (3.77%–14.87%), *Bdellovibrionota* (6.34%–16.28%),

253   *Armatimonadota* (4.52%–16.96%), RCP2-54 (2.35%–22.15%), and *Entotheonellaeota* (4.27%–21.35%),

254   which together accounted for ca. 99.55% of all bacterial sequences (Fig. 4; Table S6). The remaining

255   phyla only comprising < 1% of the total bacterial library

256   For eukaryota, 350 670 valid sequences and 202 OTUs were obtained. All sequences could be

257 assigned to one of 22 eukaryota phyla. Of these, the 12 most dominant eukaryota phyla across all samples

258 were *Ascomycota* (59.31%–96.30%), *Basidiomycota* (1.68%–35.14%), SAR_norank (0.81%–7.38%),

259 *Mucoromycota* (0.29%–1.71%), Fungi_norank (0.01%–9.50%), Eukaryota_norank (0.08%–3.04%),

260 *Schizoplasmodiida* (0.03%–1.10%), *Zoopagomycota* (0%–1.01%), Fungi_unclassified (0.03%–0.90%),

261 Eukaryota_unclassified (0.03%–0.25%), Amoebozoa_norank (0%–0.36%), and *Chytridiomycota* (0%–

262 0.46%). Among them, *Ascomycota*, *Basidiomycota*, *Mucoromycota*, Fungi_norank, *Zoopagomycota*,

263 Fungi_unclassified, and *Chytridiomycota* belonged to the fungi and constituted 88.44%–98.71% of the

264 total eukaryota library.

265

266 **3.3 Bacterial and eukaryota community composition at the two sites**

267   The PCoA done at the OTU level was used to infer the β-diversity patterning of soil bacterial and

268 eukaryotic community composition (Fig. 5). Bacterial communities of the *CE* samples strongly clustered

269 at the far right of the PC1 axis (explaining 52.96% of the total variation), unlike the *BSL* samples which

270 were well scattered along the entire PC2 axis (accounting 11.32% of the total variation). Likewise, for

271 eukaryota communities, those of the *CE* samples were clumped along the right of PC1 axis (accounting

272 for 34.49% of the total variation), whereas those of the *BSL* samples were interspersed along the length of

273 the PC2 axis (accounting for 11.32 % of the total variation).

274   The student's t-test bar plots indicated differences between the two sites (*BSL* vs. *CE* below,

275 respectively) in their bacterial and eukaryotic communities at the phylum level (Fig. 6). A total of 13

276 bacterial phyla, namely *Acidobacteria* (30.06% vs. 16.96%), *Proteobacteria* (15.23% vs. 23.6%),

277 *Chloroflexi* (12.50% vs. 6.21%), *Cyanobacteria* (2.13% vs. 0.20%), *Nitrospirota* (0.48% vs. 0.73%),

278 Bacteria_unclassified (0.43% vs. 0.69%), *Planctomycetota* (0.43% vs. 0.29%), *Deinococcota* (0.03% vs.

279 0.07%), NB1-j (0.008% vs. 0.087%), WS2 (0.064% vs. 0.0194%), GAL15 (0.0055% vs. 0.048% at CE),

280 SAR324_cladeMarine_group_B (0.00526% vs.   0.02216%), and *Dadabacteria* (0% vs. 0.023%)

281 differed significantly in their relative abundance between the *BSL* and *CE* sites (Fig. 6; Table S8). For

282 eukaryota, only Eukaryota_unclassified (0.075% vs. 0.183%), Amoebozoa_norank (0.018% vs. 0.232%),

283 and *Aphelidea* (0% vs. 0.060%), occurred in significantly different proportions between the two sites (Fig.

284   6; Table S9).

285   Mantel tests were used to discern the several environmental factors that shaped the soil bacterial and

286   eukaryota community composition across all 10 samples (Fig. 7). For bacteria, SOC ($R = 0.808$, $P =$

287   0.008) was the most critical environmental factor that individually explained the variation in soil bacterial

288   community composition, followed by soil pH ($R = 0.808$, $P = 0.008$), soil TN ($R = 0.769$, $P = 0.005$), soil

289   EC ($R = 0.710$, $P = 0.006$), soil C:N ratio ($R = 0.605$, $P=0.004$), and MBN ($R = 0.624$, $P = 0.009$) (Fig. 7;

290   Table S10). The soil eukaryota community composition was most associated with SOC ($R = 0.397$, $P =$

291   0.003), soil pH ($R = 0.341$, $P = 0.015$), soil TN ($R = 0.298$, $P = 0.013$), MBN   ($R = 0.271$, $P = 0.031$),

292   and soil EC ($R = 0.236$, $P = 0.041$) (Fig. 7; Table S10).

293

294   4. Discussion

295   *4.1 Effects of planting C. esculentus on soil microbial biomass indices and enzymatic activities*

296   Our results showed that the soil MBC, MBN, and MBP values of planted *C. esculentus* cultivated for

297   1 year were all higher than those of the control site (*BSL*), and significantly so for MBC and MBN (Fig.

298   1A; Table S3). This result is probably due to the significantly greater soil nutrient contents, especially for

299   SOC and TN, that arose in the presence of *C. esculentus* over 1 year (Table S3), likely driven by

300   accumulating organic matter derived from litter decomposition and root exudates. Generally, the sandy

301   soil in semi-arid and arid ecosystems are considered oligotrophic environments with poor nutrient status.

302   (Zhao et al., 2016). Although there are some exogenous nutrient inputs, the sandy soil still cannot

303   accumulate nutrients effectively because of its loosened soil texture that is also prone to leaching.

304   Evidently, planting and then cultivating *C. esculentus* for 1 year could improve soil nutrient conditions of

305   sandy land. An earlier study in arid and semi-arid grassland of China showed that the total biomass of soil

306   microorganisms, as well as bacterial or fungal biomass, were significantly positively correlated with the

307   SOC content (Hu et al., 2014). In other work, soil bacterial diversity was also positively correlated with

308   the TN content (Wang et al., 2015). Generally, the main factor responsible was larger concentrations of

309   key soil nutrients, especially organic matter and nitrogen, which was beneficial for the growth of soil

310   microbial populations and microbial biomass (Ralte et al., 2005).

311   Compared with the control site, the four soil enzymatic activities (BG, CBH, LAP, and NAG) under

312   planting with *C. esculentus* were hardly changed, in that only ACP was significantly decreased ($P < 0.05$)

313   (Fig. 1B; Table S1). Soil enzymes have been considered as indicators of soil quality, indicating soil

314   fertility quality and soil health quality. Nonetheless, distinct enzymes have different molecular

315   compositions and structures, and catalyze different reactions, which are affected by multiple

316   environmental factors, such as soil temperature, moisture, pH, fertilization, vegetation type, plant

317   diversity, and community structure (Fu et al., 2012; Pan et al., 2018). Although the soil nutrient status of

318   the sandy land was upgraded after the planting with *C. esculentus*, the change was not sufficient to cause

319   significant changes in soil enzymatic activities (BG, CBH, LAP, and NAG), because the treatment time

320   was only one year. By comparison, ACP are mainly produced by plant roots and microorganisms and

321   play a key role in the P cycling, an often-limiting element in terrestrial ecosystems, and its activities were

322   commonly positively correlated with soil organic matter, total nitrogen and organic phosphorus contents

323   (Margalef et al., 2021). Therefore, our results are different from conventional studies, and the specific

324   reason still needs to be confirmed through long-term positioning tests.

325

326   ***4.2 Effects of planting C. esculentus on soil microbial diversity and community composition***

327   To compare the soil microbial characteristics of bare sandy land (*BSL*, the control) and sandy land in

328   which *C. esculentus* was cultivated for 1 year (*CE*), real-time PCR and MiSeq high-throughput

329   sequencing were used in tandem to reveal differences in the soil microbial abundance, α-diversity, and

330   community composition between the two sampling sites.

331   The *q*PCR and sequencing results detected high bacterial abundance and diversity but a relatively

332   low eukaryotic abundance and diversity at the two sampling sites. For microbial abundance, twice as

333   many bacterial 16S rRNA gene copies were found in soil at *CE* than the control whereas the number of

334   eukaryota 18S rRNA gene copies was quite similar between sites (Fig. 2). The great variation in bacterial

335   16S rRNA and eukaryota 18S rRNA gene copies and their site-level disparity are probably attributable to

336   different feedback processes between bacteria and eukaryota and the soil C:N ratio, with a lower C:N

337   ratio likely benefiting more the reproduction of bacteria than fungi (Hu et al., 2001).

338   Soil bacterial phyla were dominated by *Actinobacteria*, *Acidobacteria*, *Proteobacteria*, and

339   *Chloroflexi*, while eukaryota phyla were dominated by *Ascomycota*, *Basidiomycota*, and SAR_norank

340   (Fig. 4). These phyla are widely distributed in various terrestrial ecosystems, especially in arid and semi-

341   arid regions (Baubin et al., 2019; Crits-Christoph et al., 2013; Sun et al., 2018; Zhang et al., 2019). The

342   PCoA results uncovered stark differences in soil bacterial or eukaryotic community composition of bare

343   sandy land across all its samples (Fig. 5), whereas either composition was very similar among samples

344   where planted *C. esculentus* grew for 1 year. This pattern strongly implied that the short-term presence of

345   *C. esculentus* could markedly promote the homogenization of soil bacterial and eukaryotic communities.

346   Of these, the relative abundances of several bacterial and eukaryotic phyla distinctly changed: for bacteria,

347   compared with the control, the relative abundance of *Acidobacteria* in response to *C. esculentus* planting

348   fell sharply from 30.06% to 16.96%, and that of *Proteobacteria* and *Chloroflexi* increased sharply from

349   15.23% to 23.6% and from 12.50% to 16.21%, respectively (Fig. 6). Previous studies have shown that

350   *Acidobacteria* are oligotrophic bacteria, being typically more abundant in low-nutrient soils, while

351   *Proteobacteria* are copiotrophic bacteria usually found in nutrient-rich habitats (Fierer et al., 2007; Wang

352   et al., 2017; Zeng et al., 2019). Accordingly, from our results, we may infer that the planted *C. esculentus*

353   probably enriched the soil fertility of bare sandy soil. For eukaryota, compared with the control, the

354   relative abundance of Eukaryota_unclassified in response to *C. esculentus* planting increased from 0.075%

355   to 0.18%; likewise, the relative abundances of Amoebozoa_norank and *Aphelidea* respectively increased

356   from 0.018% to 0.232% and from 0% to 0.060%.

357   Mantel tests indicated that soil microbial community composition was associated with multiple

358   edaphic drivers whose roles differed marginally between the two microbial groups (Fig. 7; Table S10).

359   For bacteria, SOC was the most fundamental environmental driver shaping the bacterial community

360   composition across all soil samples, followed by the soil pH, TN, EC, C:N ratio, and MBN. Similarly,

361   soil eukaryota community composition was mainly related to the SOC, pH, TN, MBN, and EC (Fig. 7,

362   Table S10). A predominant role for soil pH in shaping bacterial community composition has been widely

363   demonstrated at different scales and in different ecosystems (Jiao and Lu, 2020; Shen et al., 2013; Tian et

364   al., 2018; Yu et al., 2021). Furthermore, soil nutrients' content is also a limiting factor of microbial

365   activity and can pivotally impact soil microbial community distribution patterns in arid and semi-arid

366   regions (Chen et al., 2015). In our study, SOC strongly altered the community composition of both soil

367   bacteria and eukaryota, which is consistent with other studies' findings (Hu et al., 2001; Tian et al., 2018).

368

369 5. Conclusion

370   In this study, we evaluated the short-term (1 year) effects of planted *C. esculentus* on the soil

371   microbial biomass indices, enzymatic activities, and microbiome characteristics in the Horqin Sandy Land,

372   China. The presence of *C. esculentus* for 1 year is capable of inducing the differential accumulation of

373   SOC and TN, thereby increasing the soil C:N ratio. Furthermore, *C. esculentus* can promote three

374   microbial biomass indices (MBC, MBN, and MBP) but it has very little impact on four enzymes' (BG,

375   CBH, LAP, and NAG) activities. Moreover, planting with *C. esculentus* significantly increases the

376   richness and diversity of soil bacteria rather than eukaryota in sandy land, while reducing and augmenting

377   the relative abundance of *Acidobacteria* and *Proteobacteria*, respectively, suggesting their potential use

378   as bioindicators of soil nutrient-rich conditions. Overall, our findings demonstrate that cultivating *C.*

379   *esculentus* for just 1 year could improve the nutrient status and microbial characteristics of sandy soils in

380   a semi-arid region.

381

382 Author Contributions

383   Sample collection: YLD.

384   Data curation: YLD, CL, JHZ.

385   Funding acquisition: YLD

386   Methodology: YLD, CL.

387   Project administration: YLD

388   Writing-original draft: YLD, WR, and YL.

389   Writing-review & editing: YLD, WR, and YL.

390   All authors contributed to the article and approved the submitted version.

391

Funding

393   This research work was supported by the National Key R&D Program of China (grant no.
394 2019YFC0507602) and the "Light of West China" Program of the Chinese Academy of Sciences
395 (E0290501).

396

Data statement

398   The following information was supplied regarding data availability: The raw measurements are
399 available as a Supplemental File.

400

Declaration of competing interest

402   The authors declare no conflicts of interest. The authors Jianhua Zhao and Chun Luo were employed
403 by Shanghai Majorbio Bio-Pharm Technology Co. Ltd. The author Yang Liu is employed by Gansu
404 Institute of Architectural Design and Research Company. The remaining authors confirm the research was
405 conducted in the absence of any commercial or financial relationships that could be construed as a
406 potential conflict of interest. The funders had no role in the design of the study; nor, in the collection,
407 analyses, or interpretation of data, in the writing of the manuscript, or in the decision to publish the results.

408

Figure legends

409

410   **Fig. 1. Soil microbial biomass indices (MBC, MBN, MBC/MBN ratio, and MBP) (A) and soil enzyme**

411   **activities (BG, CBH, LAP, NAG, and ACP) (B) in the topsoil (to a depth of 20 cm) at the two sampling**

412   **sites**. *BSL*: bare sandy land; *CE*: sandy land where *Cyperus esculentus* was cultivated for 1 year. Bars are the

413   mean ± SD, *n* = 5. *MBC*: microbial biomass carbon; *MBN*: microbial biomass nitrogen; *MBP*: microbial

414   biomass phosphorus; *BG*: 1,4-glucosidase; *CBH*: cellobiohydrolase; *LAP*: leucine aminopeptidase; *NAG*: β-1,

415   4-N-acetaminoglycosidase; *ACP*: acid phosphatase. Significant levels (ANOVA followed by LSD test): * *P* <

416   0.05; ** *P* < 0.01; *** *P* < 0.001.

417   **Fig. 2. Comparison of the 16S rRNA gene (for bacteria) and 18 rRNA gene (for eukaryota) copy**

418   **numbers from the soils at the two sampling sites as determined by *q*PCR.** *BSL*: bare sandy land; *CE*: sandy

419   land where *Cyperus esculentus* was cultivated for 1 year. Bars are the mean ± SD, *n* = 5. Significant levels

420   (ANOVA followed by LSD test): * *P* < 0.05.

421   **Fig. 3. The α-diversity (Chao and Shannon indices) of the microbial community between the two sites.**

422   *BSL*: bare sandy land; *CE*: sandy land where *Cyperus esculentus* was cultivated for 1 year. Bars are the mean ±

423   SD, *n* = 5. Significant levels (ANOVA followed by LSD test): * *P* < 0.05.

424   **Fig. 4. Relative abundances of the bacterial and eukaryota community members at the phylum level**

425   **across all 10 soil samples.** *BSL*: bare sandy land; *CE*: sandy land in which *Cyperus esculentus* was cultivated

426   for 1 year.

427   **Fig. 5. Results of the principal co-ordinates analysis (PC1 and PC2) for the soil bacterial and eukaryotic**

428   **communities at the two sampling sites.** *BSL*: bare sandy land; *CE*: sandy land in which *Cyperus esculentus*

429   was cultivated for 1 year.

430   **Fig. 6. Proportions at the phylum level for the two groups and tests for their significant differences.** *BSL*:

431   bare sandy land; *CE*: sandy land in which *C. esculentus* was cultivated for 1 year.

432   **Fig. 7. Pairwise comparisons of environmental factors with soil bacterial or eukaryota community**

433   **composition, for which a color gradient denotes Pearson's correlation coefficient.**

434   *SOC:* soil organic carbon; *TN:* total nitrogen; *TP:* total phosphorus; *EC:* electric conductivity; *MBC:* microbial

435   biomass carbon; *MBN:* microbial biomass nitrogen; *MBP:* microbial biomass phosphorus. Pearson's *r* > 0

436 indicates a positive correlation and $r < 0$ indicates a negative correlation. The boxed-edge width corresponds to

437 the distance dependence of Mantel's R statistic, whose statistical significance was based on $n = 9999$

438 permutations. An inner square's size is proportional to the strength of Mantel's R correlation. The color of the

439 curved lines indicates the correlation strength between bacterial or eukaryota community composition and the

440 environmental factors.

441

442 **References**

443 **Allison SD, Jastrow JD. 2006.** Activities of extracellular enzymes in physically isolated fractions of restored

444 grassland soils. *Soil Biology & Biochemistry* **38:** 3245-3256. DOI 10.1016/j.soilbio.2006.04.011.

445 **Asare PA, Kpankpari R, Adu MO, Afutu E, Adewumi AS. 2020.** Phenotypic characterization of tiger nuts

446 (*Cyperus esculentus*) from major growing areas in Ghana. *The Scientific World Journal* 7232591.

447 **Baubin C, Farrell AM, Ovíek A, Ghazaryan L, Gillor O. 2019.** Seasonal and spatial variability in total and active

448 bacterial communities from desert soil. *Pedobiologia*. **74:** 7-14. DOI 10.1016/j.pedobi.2019.02.001.

449 **Brunner K, Peterbauer CK, Mach RL, Lorito M, Zeilinger S, Kubicek CP. 2003.** The Nag1 N-

450 acetylglucosaminidase of *Trichoderma atroviride* is essential for chitinase induction by chitin and of major

451 relevance to biocontrol. *Current Genetics*. **43:** 289-295. DOI10.1007/s00294-003-0399-y.

452 **Bünemann E, Bongiorno G, Bai Z, Creamer RE, Brussaard L. 2018.** Soil quality - A critical review. *Soil

453 Biology & Biochemistry* **120:** 105-125. DOI 10.1016/j.soilbio.2018.01.030.

454 **Caldwell B. 2005.** Enzyme activities as a component of soil biodiversity: A review. *Pedobiologia*. **49:** 637-644.

455 DOI 10.1016/j.pedobi.2005.06.003.

456 **Chen DM, Mi J, Chu PF, Cheng JH, Zhang LX, Pan QM, Xie YC, Bai YF. 2015.** Patterns and drivers of soil

457 microbial communities along a precipitation gradient on the Mongolian Plateau. *Landscape Ecology* **30:** 1669-

458 1682. DOI 10.1007/s10980-014-9996-z.

459 **Chen SF, Zhou YQ, Chen YR, Gu J. 2018.** fastp: an ultra-fast all-in-one FASTQ preprocessor. *Bioinformatics* **34:**

460 884-890. DOI 10.1093/bioinformatics/bty560.

461 **Crits-Christoph A, Robinson CK, Barnum T, Fricke WF, Davila AF, Jedynak B, McKay CP Di Ruggiero J.**

462 **2013** Colonization patterns of soil microbial communities in the Atacama Desert. *Microbiome* **1:** 28. DOI

463 10.1186/2049-2618-1-28.

464 **Dennis KL, Wang Y, Blatner NR, Wang S, Saadalla A, Trudeau E. 2013.** Adenomatous polyps are driven by

465 microbe-instigated focal inflammation and are controlled by IL-10–producing T Cells. *Cancer Research* **73:**

466 5905-5913. DOI 10.1158/0008-5472.CAN-13-1511.

467 **Dick WA, Cheng L, Wang P. 2000.** Soil acid and alkaline phosphatase activity as pH adjustment indicators. *Soil

468 Biology & Biochemistry* 32: 1915-1919. DOI 10.1016/S0038-0717(00)00166-8.

469 **Dirks RC, Singh M, Potter GS, Sobotka LG, Schaefer J. 2012.** Carbon partitioning in soybean (Glycine max)
470   leaves by combined 11C and 13C labeling. *New Phytologist* **196:** 1109-1121. DOI 10.1111/j.1469-
471   8137.2012.04333. x.

472 **Edgar RC. 2013.** UPARSE: highly accurate OTU sequences from microbial amplicon reads. *Nature Methods* **10:**
473   996-998. DOI 10.1038/nmeth.2604.

474 **Fierer N, Bradford MA, Jackson RB. 2007.** Toward an ecological classification of soil bacteria. *Ecology* **88:**
475   1354-1364. DOI 10.1890/05-1839.

476 **Fu QL, Liu C, Ding NF, Lin YC, Guo B, Luo JF, Wang HH. 2012.** Soil microbial communities and enzyme
477   activities in a reclaimed coastal soil chronosequence under rice–barley cropping. *Journal of Soils and*
478   *Sediments* **12:** 1134-1144. DOI 10.1007/s11368-012-0544-7.

479 **Haan RD, Kroukamp H, Zyl JHDV, Zyl WHV. 2013.** Cellobiohydrolase secretion by yeast: Current state and
480   prospects for improvement. *Process Biochemistry* **48:** 1-12. DOI 10.1016/j.procbio.2012.11.015.

481 **Hu S, Chapin FS, Firestone MK, Field CB, Chiariello NR. 2001.** Nitrogen limitation of microbial decomposition
482   in a grassland under elevated CO_2. *Nature* **409:** 188-191. DOI 10.1038/35051576.

483 **Hu YJ, Dan X, Veresoglou SD, Chen FL, Chen YL, Hao ZP, Zhang X. 2014.** Soil organic carbon and soil
484   structure are driving microbial abundance and community composition across the arid and semi-arid grasslands
485   in northern China. *Soil Biology & Biochemistry* **77:** 51-57. DOI 10.1016/j.soilbio.2014.06.014.

486 **Hu YG, Zhang ZS, Huang L, Qi Q, Liu LC, Zhao Y, Wang ZR, Zhou HK, Lv XY, Mao ZC, Yang YF, Zhou**
487   **JZ, Kardol P. 2019.** Shifts in soil microbial community functional gene structure across a 61-year desert
488   revegetation chronosequence. *Geoderma* **347:** DOI 126-134. 10.1016/j.geoderma.2019.03.046.

489 **Jenkinson DS, Ladd JN. 1981.** Microbial biomass in soil: Measurement and turnover. Soil biochemistry 5.

490 **Jiao S, Lu YH. 2020.** Soil pH and temperature regulate assembly processes of abundant and rare bacterial
491   communities in agricultural ecosystems. *Environment Microbiology* **22:** 1052-1065. DOI 10.1111/1462-
492   2920.14815.

493 **Joergensen RG. 1996.** The fumigation-extraction method to estimate soil microbial biomass: Calibration of the
494   kEC value. *Soil Biology & Biochemistry* **28:** 25-31. DOI 10.1016/0038-0717(95)00102-6.

495 **Lange M, Eisenhauer N, Sierra CA, Bessler H, Engels C, Griffiths RI, Mellado-Vázquez PG, Malik AA, Roy**
496   **J, Scheu S, Steinbeiss S, Thomson BC, Trumbore SE, Gleixner G. 2015.** Plant diversity increases soil
497   microbial activity and soil carbon storage. *Nature Communications* **6:** 6707. DOI 10.1038/ncomms7707.

498 **Ma J, Rabin SS, Anthoni P, Bayer AD, Nyawira SS, Olin S. 2022.** Assessing the impacts of agricultural
499   managements on soil carbon stocks, nitrogen loss, and crop production – a modelling study in eastern Africa.
500   *Biogeosciences* **19:** 2145-2169. DOI 10.5194/bg-2021-352.

501 **Margalef O, Sardans J, Maspons J, Molowny-Horas R, Fernández-Martínez M, Janssens IA, Richter A, Ciais**
502   **P, Obersteiner M, Peñuelas J. 2021.** The effect of global change on soil phosphatase activity. *Global Change*
503   *Biology* **27:** 5989-6003. DOI 10.1111/gcb.15832.

504 **Muhammad I, Wang J, Sainju UM, Zhang SH, Zhao FZ, Khan A. 2021.** Cover cropping enhances soil

505 microbial biomass and affects microbial community structure: A meta-analysis. *Geoderma* 381: 114696. DOI
506 10.1016/j.geoderma.2020.114696.

507 **Neilson JW, Quade J, Ortiz M, Nelson WM, Legatzki A, Tian F, LaComb F, Betancourt JL, Wing RA,**
508 **Soderlund CA, Maier RM. 2012.** Life at the hyperarid margin: novel bacterial diversity in arid soils of the
509 Atacama Desert, Chile. *Extremophiles* **16:** 553-566. DOI 10.1007/s10482-013-9911-7.

510 **Niu YY, Duan YL, Li YQ, Wang XY, Chen Y, Wang LL. 2021.** Soil microbial community responses to short-
511 term nitrogen addition in China's Horqin Sandy Land. *PLoS ONE* **16:** e0242643. DOI
512 10.1371/journal.pone.0242643.

513 **Oderinde RA, Tairu OA. 1988.** Evaluation of the properties of yellow nutsedge (*Cyperus esculentus*) tuber oil.
514 *Food Chemistry* **28(3):** 233-237. DOI 10.1016/0308-8146(88)90055-6.

515 **Pan FJ, Zhang W, Liang YM, Liu SJ, Wang KL. 2018.** Increased associated effects of topography and litter and
516 soil nutrients on soil enzyme activities and microbial biomass along vegetation successions in karst ecosystem,
517 southwestern China. *Environmental Science and Pollution Research* **25:** 16979-16990. DOI 10.1007/s11356-
518 018-1673-3.

519 **Powlson DS, Hirsch PR, Brookes PC. 2001.** The role of soil microorganisms in soil organic matter conservation in
520 the tropics. *Nutrient Cycling in Agroecosystems* **61:** 41-51. DOI 10.1023/A:1013338028454.

521 **Quast C, Pruesse E, Yilmaz P, Gerken J, Schweer T, Yarza P, Peplies J, Glockner FO. 2013.** The SILVA
522 ribosomal RNA gene database project: improved data processing and web-based tools. *Nucleic Acids Research*
523 **41:** 590-596. DOI 10.1093/nar/gks1219.

524 **Ralte V, Pandey HN, Barik SK, Tripathi RS, Prabhu SD. 2005.** Changes in microbial biomass and activity in
525 relation to shifting cultivation and horticultural practices in subtropical evergreen forest ecosystem of north-east
526 India. *Acta Oecologica* **28:** 163-172. DOI 10.1016/j.actao.2005.04.001.

527 **Rousk J, Bååth E, Brookes PC, Lauber CL, Lozupone C, Caporaso JG, Knight R, Fierer N. 2010.** Soil
528 bacterial and fungal communities across a pH gradient in an arable soil. *The ISME Journal* **4:** 1340-1351. DOI
529 10.1038/ismej.2010.58.

530 **Schloss PD, Westcott SL, Ryabin T, Hall JR, Hartmann M, Hollister EB, Lesniewski RA, Oakley BB, Parks**
531 **DH, Robinson CJ, Sahl JW, Stres B, Thallinger GG, Van Horn DJ, Weber CF. 2009.** Introducing mothur:
532 opensource, platform-independent, community-supported software for describing and comparing microbial
533 communities. *Applied and Environmental Microbiology* **75:** 7537-7541. DOI 10.1128/AEM.01541-09.

534 **Sha RN, Yu MH, Ding GD, Zhao YY, Sai K, Zhang GX. 2022.** Shelter efficiency of conservation tillage model in
535 *Cyperus esculentus* in sandy farmland. *Journal of Arid Land Resources and Environment* 36: 87-94. DOI
536 10.13448/j.cnki.jalre.2022.096 (In Chinese).

537 **Shao TY, Zhao JJ, Liu AH, Long XH, Rengel Z. 2020.** Effects of soil physicochemical properties on microbial
538 communities in different ecological niches in coastal area. *Applied Soil Ecology* **150:** 103486. DOI
539 10.1016/j.apsoil.2019.103486.

540 **Shen CC, Xiong JB, Zhang HY, Feng YZ, Lin XG, Li XY, Liang WJ, Chu HY. 2013.** Soil pH drives the spatial

541   distribution of bacterial communities along elevation on Changbai Mountain. *Soil Biology & Biochemistry* **57:**
542   204-211. DOI 10.1016/j.soilbio.2012.07.013.

543   **Sparling GP, Pankhurst C, Doube B, Gupta V. 1997.** Soil microbial biomass, activity and nutrient cycling as
544   indicators of soil health. Biological indicators of soil health. Wallingford; New York (USA): CAB International
545   97-119.

546   **Sun Y, Shi YL, Wang H, Zhang T, Yu LY, Sun H, Zhang YQ. 2018.** Diversity of bacteria and the characteristics
547   of actinobacteria community structure in Badain Jaran Desert and Tengger Desert of China. *Frontiers in*
548   *Microbiology* **9:** 1068. DOI 10.3389/fmicb.2018.01068.

549   **Tian J, He NP, Hale L, Niu SL, Yu GR, Liu Y, Blagodatskaya E, Kuzyakov Y, Gao Q, Zhou JZ. 2018.** Soil
550   organic matter availability and climate drive latitudinal patterns in bacterial diversity from tropical to cold
551   temperate forests. *Functional Ecology* **32:** 61-70. DOI 10.1111/1365-2435.12952.

552   **Wang JC, Song Y, Ma TF, Raza W, Li J, Howland JG, Huang QW, Sheng QR. 2017.** Impacts of inorganic and
553   organic fertilization treatments on bacterial and fungal communities in a paddy soil. *Applied Soil Ecology* **112:**
554   42-50. DOI 10.1016/j.apsoil.2017.01.005.

555   **Wang XB, Van Nostrand, JD, Deng Y, Lv XT, Wang C, Zhou JZ, Han XG. 2015.** Scale-dependent effects of
556   climate and geographic distance on bacterial diversity patterns across northern China's grasslands. *FEMS*
557   *Microbiology Ecology* **91:** 12. DOI 10.1093/femsec/fiv133.

558   **Yu J, Yin Q, Niu JM, Yan ZJ, Wang H, Wang YQ, Chen DM. 2022.** Consistent effects of vegetation patch type
559   on soil microbial communities across three successional stages in a desert ecosystem. *Land Degradation &*
560   *Development* **33:** 1552-1563. DOI 10.1002/ldr.4194.

561   **Yu WJ, Lawrence NC, Sooksa-nguan T, Smith SD, Tenesaca C, Howe AC, Hall SJ. 2021.** Microbial linkages to
562   soil biogeochemical processes in a poorly drained agricultural ecosystem. S*oil Biology and Biochemistry*
563   **156:** 108228. DOI 10.1016/j.soilbio.2021.108228.

564   **Zeng QC, An SS, Liu Y, Wang HL, Wang Y. 2019.** Biogeography and the driving factors affecting forest soil
565   bacteria in an arid area. *Science of The Total Environment* **680:** 124-131. DOI 10.1016/j.scitotenv.2019.04.184.

566   **Zhang KP, Shi Y, Cui XP, Yue P, Li KH, Liu XJ, Tripathi BM, Chu HY, Lozupone C. 2019.** Salinity is a key
567   determinant for soil microbial communities in a desert ecosystem. *mSystems* **4:** e00225-18. DOI
568   10.1128/mSystems.00225-18.

569   **Zhang XT, Wu XQ. 2022.** Cultivation and production potential evaluation of Cyperus esculentus L. in marginal
570   land of Inner Mongolia. *Transactions of the Chinese Society of Agricultural Engineering* **38:** 289-295. DOI
571   10.11975/j.issn.1002-6819.2022.02.032. (In Chinese).

572   **Zhao CC, Miao Y, Yu CD, Zhu LL, Wang F, Jiang L, Hui DF, Wan SQ. 2016.** Soil microbial community
573   composition and respiration along an experimental precipitation gradient in a semiarid steppe. *Scientific*
574   *Reports* **6:** 24317. DOI 10.1038/srep24317.

Figure 1

Soil microbial biomass indices (MBC, MBN, MBC/MBN ratio, and MBP) (A) and soil enzyme activities (BG, CBH, LAP, NAG, and ACP) (B) in the topsoil (to a depth of 20 cm) at the two sampling sites

BSL : bare sandy land; *CE*: sandy land where *Cyperus esculentus* was cultivated for 1 year.

Bars are the mean ± SD, *n* = 5. *MBC* : microbial biomass carbon; *MBN*: microbial biomass

nitrogen; *MBP*: microbial biomass phosphorus; *BG*: 1,4-glucosidase; *CBH*: cellobiohydrolase;

LAP: leucine aminopeptidase; *NAG*: β-1, 4-N-acetaminoglycosidase; *ACP*: acid phosphatase.

Significant levels (ANOVA followed by LSD test): * *P* < 0.05 ; ** *P* < 0.01 ; *** *P* < 0.001.
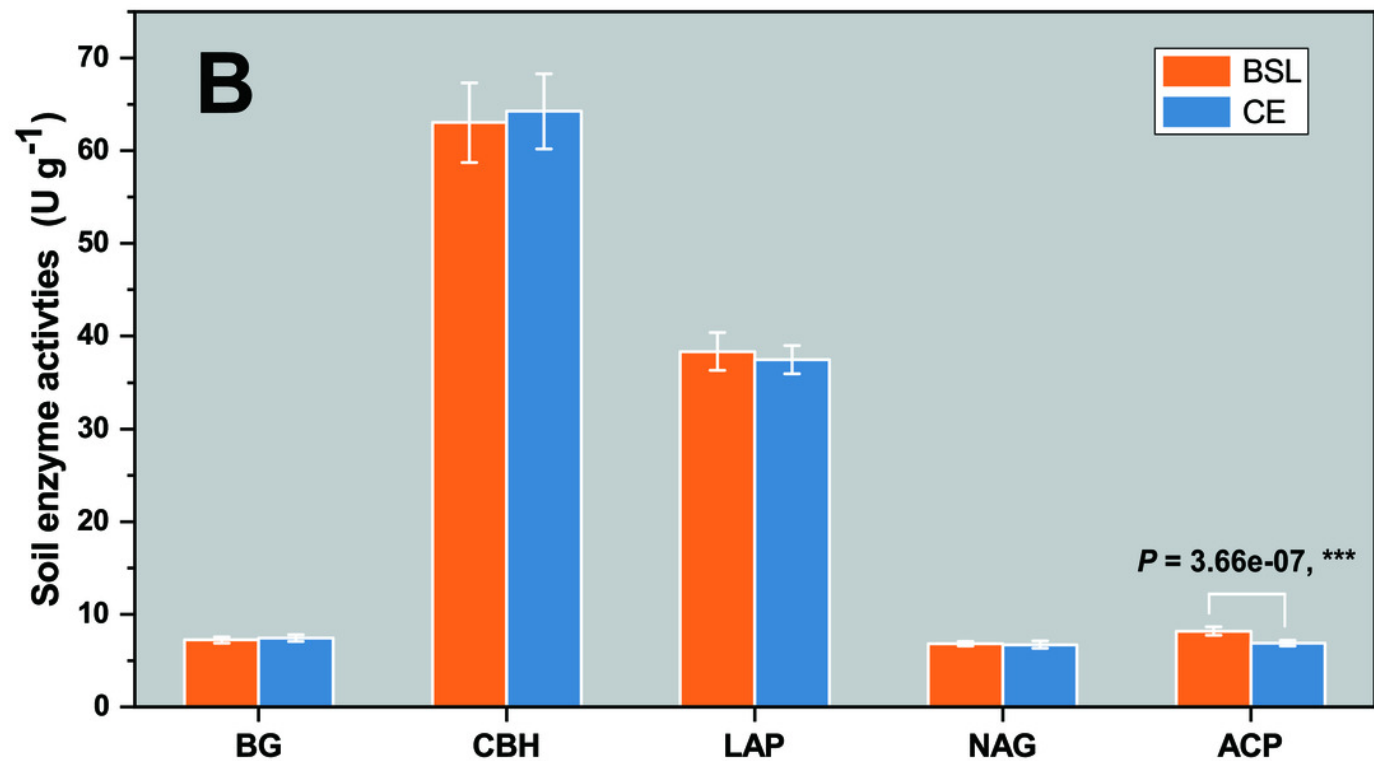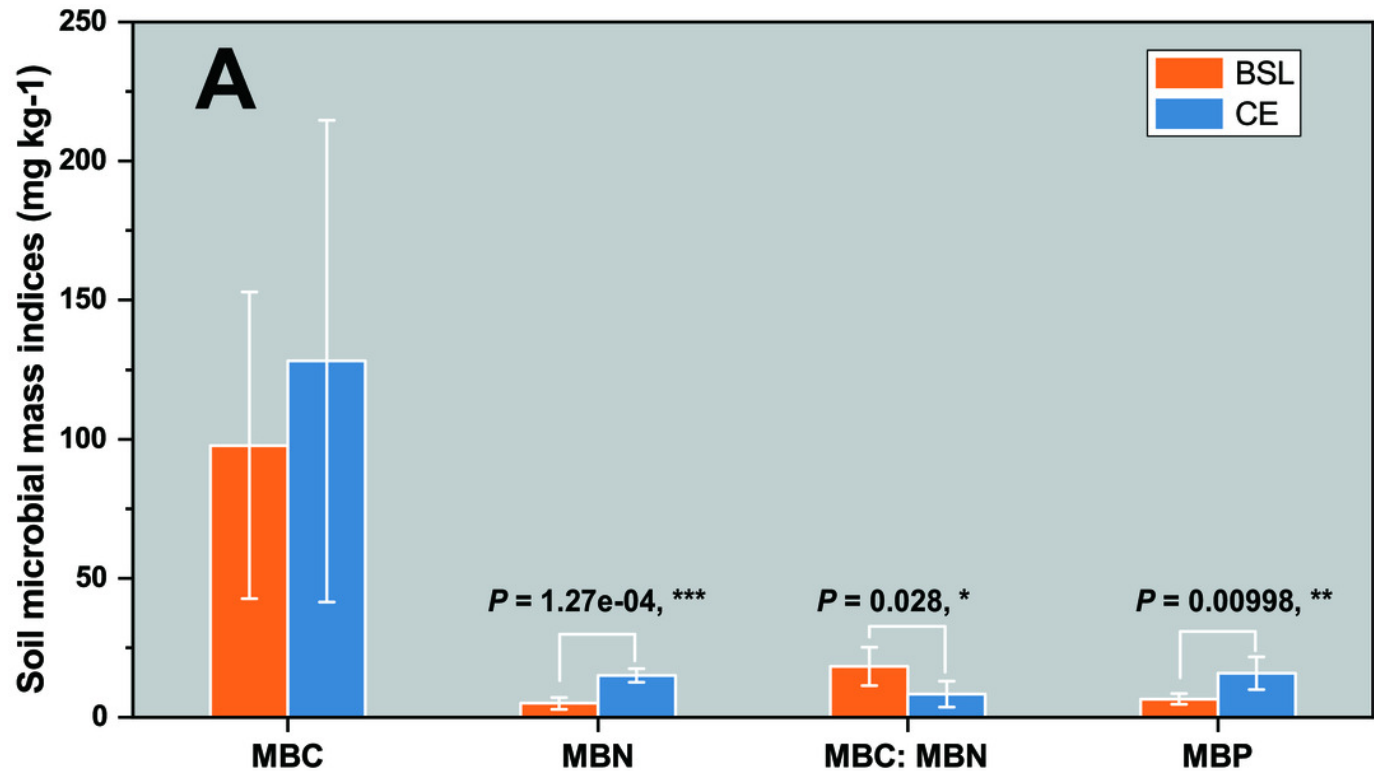
Figure 2

Fig. 2. Comparison of the 16S rRNA gene (for bacteria) and 18 rRNA gene (for eukaryota) copy numbers from the soils at the two sampling sites as determined by *q*PCR.

BSL: bare sandy land; *CE*: sandy land where *Cyperus esculentus* was cultivated for 1 year.

Bars are the mean ± SD, *n* = 5. Significant levels (ANOVA followed by LSD test): * *P* < 0.05.
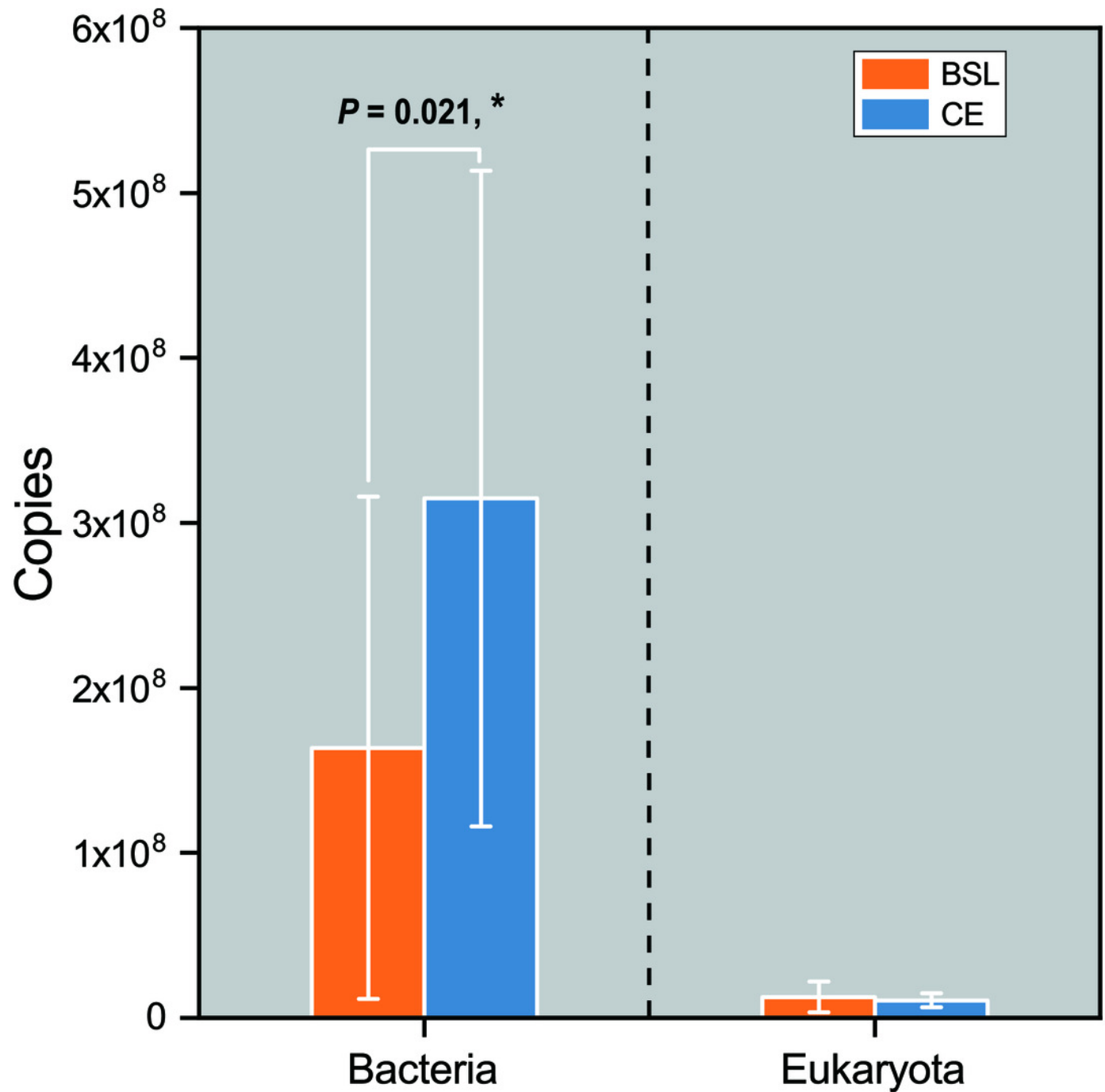
Figure 3

The α-diversity (Chao and Shannon indices) of the microbial community between the two sites.

BSL: bare sandy land; *CE*: sandy land where *Cyperus esculentus* was cultivated for 1 year. Bars are the mean ± SD, *n* = 5. Significant levels (ANOVA followed by LSD test): * *P* < 0.05.
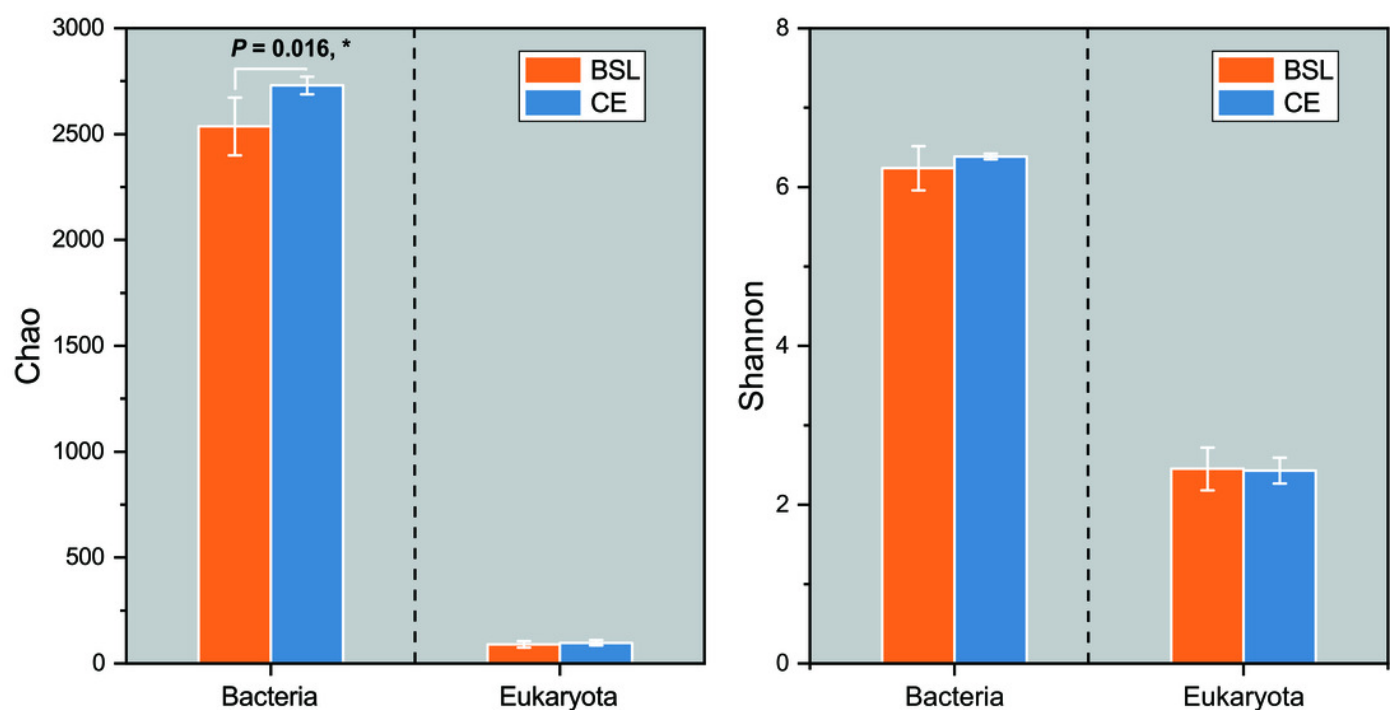
Figure 4

Relative abundances of the bacterial and eukaryota community members at the phylum level across all 10 soil samples.

BSL: bare sandy land; *CE*: sandy land in which *Cyperus esculentus* was cultivated for 1 year.
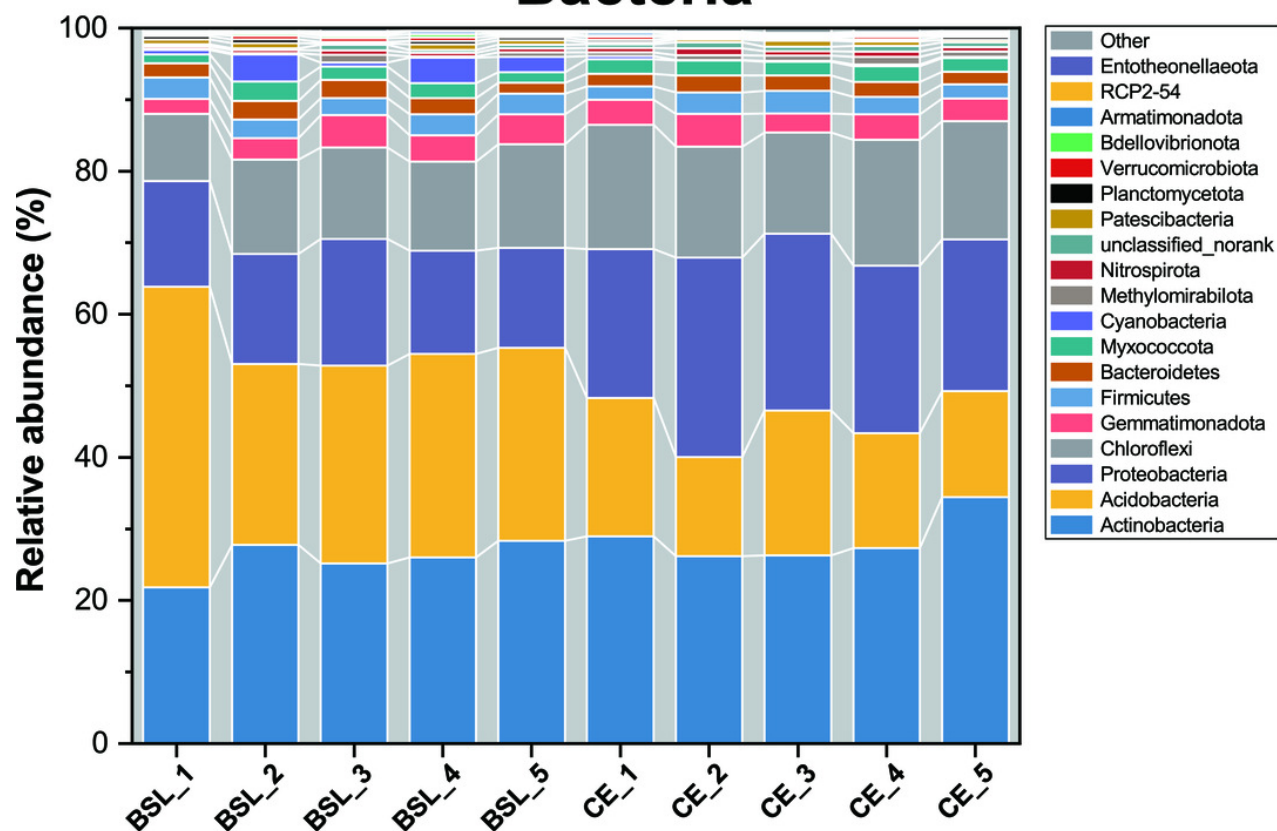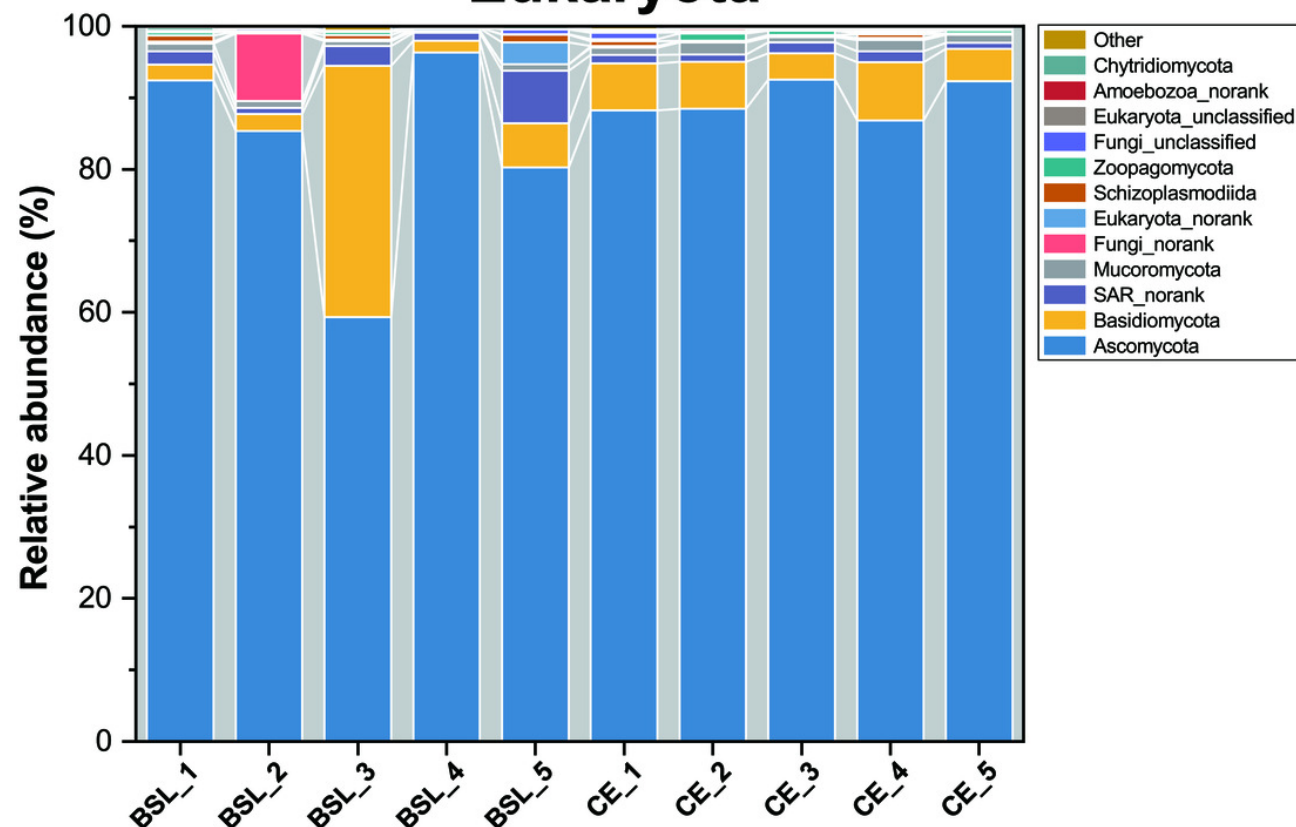
Figure 5

Results of the principal co-ordinates analysis (PC1 and PC2) for the soil bacterial and eukaryotic communities at the two sampling sites.

BSL: bare sandy land; *CE*: sandy land in which *Cyperus esculentus* was cultivated for 1 year.
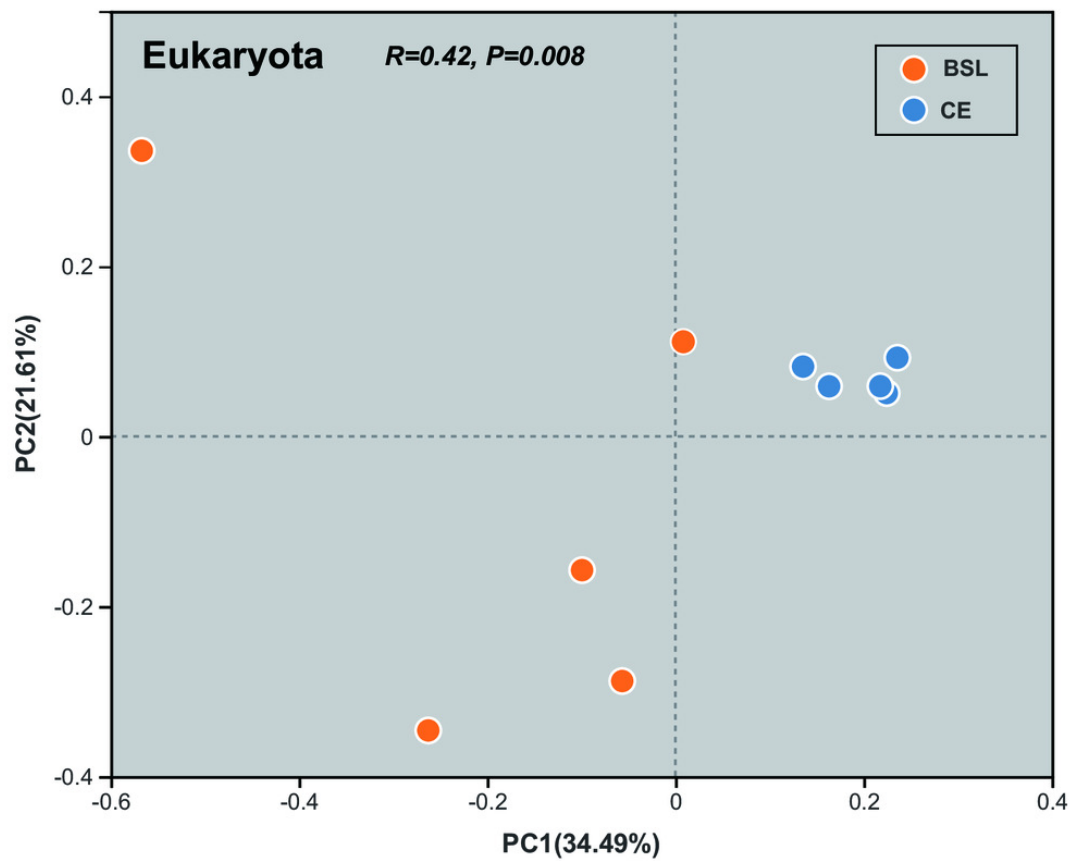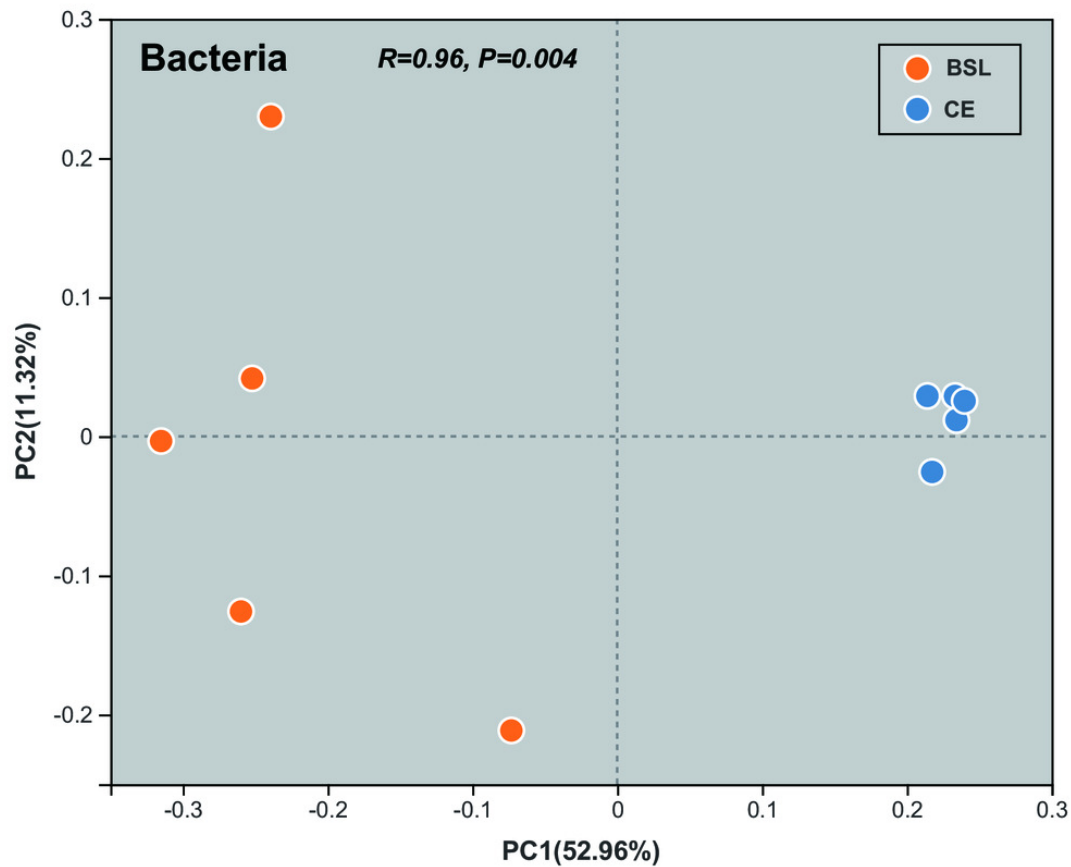
Figure 6

Proportions at the phylum level for the two groups and tests for their significant differences.

BSL: bare sandy land ; *CE*: sandy land in which *C. esculentus* was cultivated for 1 year.
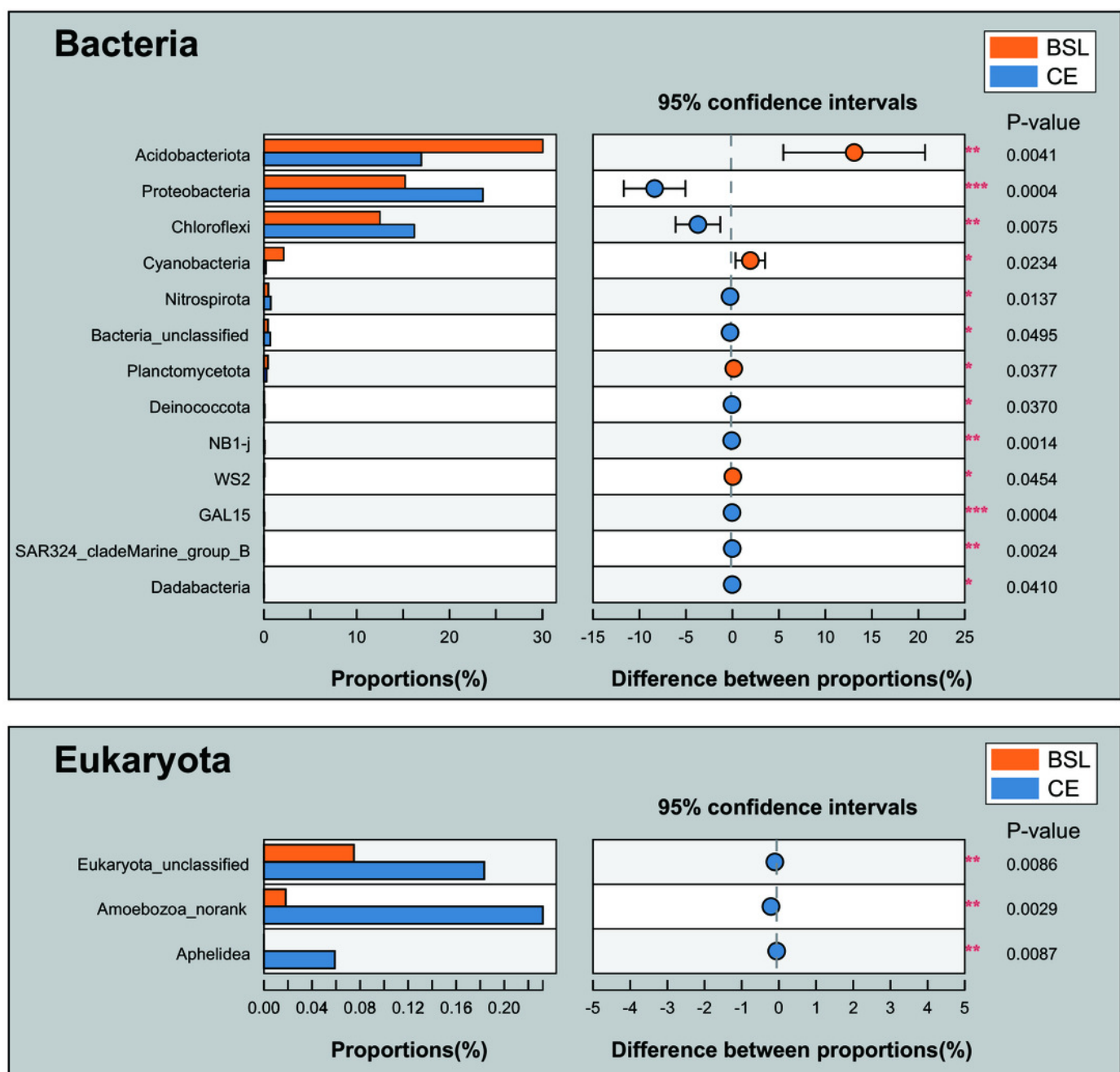
Figure 7

Pairwise comparisons of environmental factors with soil bacterial or eukaryota community composition, for which a color gradient denotes Pearson's correlation coefficient.

SOC: soil organic carbon; *TN:* total nitrogen; *TP:* total phosphorus; *EC:* electric conductivity; *MBC:* microbial biomass carbon; *MBN:* microbial biomass nitrogen; *MBP:* microbial biomass phosphorus. Pearson's *r* > 0 indicates a positive correlation and *r* < 0 indicates a negative correlation. The boxed-edge width corresponds to the distance dependence of Mantel's *R* statistic, whose statistical significance was based on *n* = 9999 permutations. An inner square's size is proportional to the strength of Mantel's R correlation. The color of the curved lines indicates the correlation strength between bacterial or eukaryota community composition and the environmental factors.